

Vlasov kinetic modeling and studies of plasma transport during ELM in Tokamak

C. Wang and S. Van Loo

Department of Applied Physics, Ghent University, Ghent, Belgium

Motivation Recently, a Vlasov kinetic code named KOBRA, using adaptive mesh refinement (AMR)[1] was developed to model plasma transport from mid-plane to divertor targets during edged localized models (ELM). The code was benchmarked against another Vlasov code, VS-PEA[2], which employs a uniform grid, thereby verifying the accuracy of KOBRA. Moreover, owing to AMR, KOBRA achieves a average memory reduction of 30% – 40% and approximately a twofold increase in computational speed compared with the uniform grid.

In ELM simulations, we notice that there are two important characteristic scales on space and time which are closely related to numerical stability and computational efficiency. The first is the plasma sheath width l_{sheath} near the divertor targets. The sheath forms after the ELM filament propagates towards the divertor. Strong charge separation in this region induces significant numerical stiffness in the electric field calculation. The second characteristic scale is the time required for the ELM plasma to enter a quasi-neutral state, denoted by (τ_{quasi}). This process is very rapid and typically occurs before the filament reaches targets. After τ_{quasi} , the influence of the self-consistent electric field on ions becomes negligible, and the ions behave almost as free streaming particles. It suggests that disabling the electric field solver in KOBRA after τ_{quasi} could significantly reduce the computational cost if only considering physics related to ions.

Therefore, the quantitative analysis of l_{sheath} and τ_{quasi} is essential for mitigating numerical instability and reducing computational cost. Furthermore, such analysis provides deeper insight into the spatial and temporal characteristics of ELM filament transport in the scrape-off layer.

KOBRA Unlike the default version of KOBRA, which solves the standard Poisson equation, the version used in this work is capable of handling the quasi-neutral regime, where the numerical domain is much larger than the Debye length, through the introduction of a modified Poisson equation [1]. KOBRA now employs a Strang splitting scheme[3]for the Vlasov equation (1).

$$\partial_t f_j + v_x \partial_x f_j - \frac{q_j}{m_j} \frac{\partial \phi}{\partial x} \frac{\partial f_j}{\partial v_x} = 0 \quad (1)$$

Here, f_j is phase-space distribution function of species j denoted by H^+ and e^- . The equation (1) is split into advection in physical space and velocity space, which are solved alternately.

Within one full time step, the spatial advection is advanced with half time steps, while the velocity advection uses a full time step. To solve for the potential, the asymptotic-preserving (AP) scheme[4] which solves a modified Poisson equation is implemented in KOBRA. This scheme allows the spatial and temporal resolutions, Δx and Δt , to exceed the limitations imposed by the Debye length and the inverse plasma frequency, thereby significantly improving computational efficiency. Regarding the AMR strategy, grid refinement is performed after a full time step. For initial condition, the spatial distribution is assumed to follow a Gaussian profile, while the velocity distribution is initialized using a Maxwellian distribution.

Simulation results Firstly, we identify τ_{quasi} by disabling electric field solver at three different times: $1\tau_e$, $5\tau_e$ and $10\tau_e$, where τ_e is electron transit time. Figure 1 shows the ion flux on divertor targets after the electric field is disabled at these three times. The normal solution and free streaming solution are also shown for comparison. In fig.1, the peak ion flux shifts from $(30\tau_e, 0.07n_{ped}v_{TH+})$ to $(21\tau_e, 0.11n_{ped}v_{TH+})$ as the duration of electric field influence on ions increases. The peak increases by approximately 57%, while the corresponding peak time is advanced by about 33%. It indicates the electric field plays a crucial role in ELM filament transport. Consequently, the free streaming model ignoring the electric field may lead to inaccurate predictions of ion flux and the associated heat flux relevant to target melting and erosion.

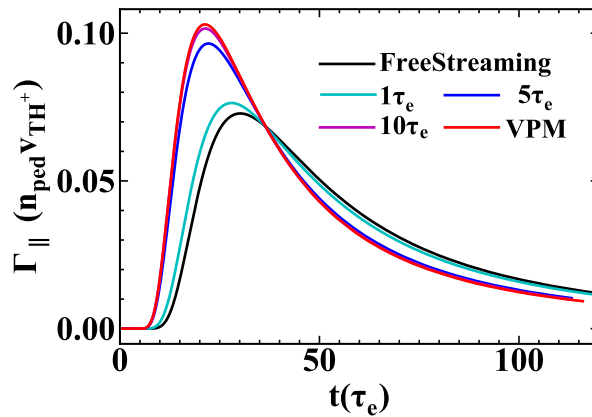


Figure 1: Ion flux on target plates after disabling electric field at three different time: $1\tau_e$, $5\tau_e$ and $10\tau_e$ and the normal ion flux and free streaming ion flux are also shown for comparison.

According to the standard KOBRA simulation, the ELM filament reaches the divertor targets at approximately $\sim 7\tau_e$. This timescale is much shorter than that of the full ELM process, which lasts about $\sim 160\tau_e$. Before the filament reaches the targets, its dynamics is dominated by self-consistent electric field because the sheath near targets has not formed yet. During this stage, this field significantly accelerates on ions, leading to an increase in the flux peak and an

earlier peak time, as observed for the $1\tau_e$ and $5\tau_e$ in fig.1. After the filament reaches targets, the peak ion flux increase slowly, and the corresponding peak time changes very little as the time for closing field solver off is delayed. This behavior suggests that the electric field after $7\tau_e$ is significantly weaker than that during the early transport stage before the filament at the targets. As a result, ions enter into free streaming state. Especially, the ion flux obtained by disabling the field at $10\tau_e$ agrees closely with the normal flux, with differences of less than $\ll 1\%$, near the peaks. This observation further indicates that the sheath electric field is not as essential as self-consistent electric field during the early transport phase. Therefore, for quantities relevant to divertor lifetime, we can obtain the nearly identical results even after turning off the field solver at $10\tau_e$, while substantially reducing the computational cost.

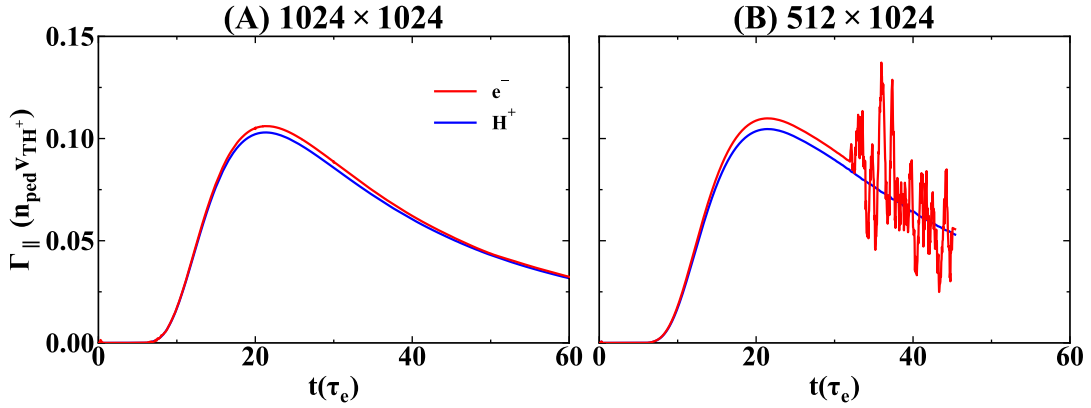


Figure 2: Ion and electron fluxes at the target plates for two different grid resolutions: (A) 1024×1024 and (B) 512×1024 .

Next, the sheath width l_{sheath} is investigated using two different resolutions, 1024×1024 and 512×1024 , corresponding to spatial resolutions of approximately $2\lambda_D$ and $4\lambda_D$, respectively. Figure 2 presents the ion and electron fluxes at the targets obtained with these two resolutions. Significant numerical oscillations are observed after the peak in the $4\lambda_D$ case. Figure 3 shows the electron distribution functions and the corresponding electric fields at $25\tau_e$ for both resolutions. Compared with the $2\lambda_D$ case, strong oscillations in the electric field E_x are observed near the targets when $\Delta x = 4\lambda$. These oscillations substantially distort the electron distribution in the sheath. The perturbed electron distribution further affects the charge density and the resulting electric field, causing the oscillations to propagate into the quasi-neutral plasma region. In contrast, when $\Delta x = 2\lambda$, the sheath region is sufficiently resolved and no noticeable oscillations are observed. This result suggests that the sheath width is very small, approximately $2\lambda - 3\lambda$ which is consistent with the typical scale of a Debye sheath. Therefore, sufficient resolution of the sheath is essential to avoid numerical instability associated with an unresolved sheath.

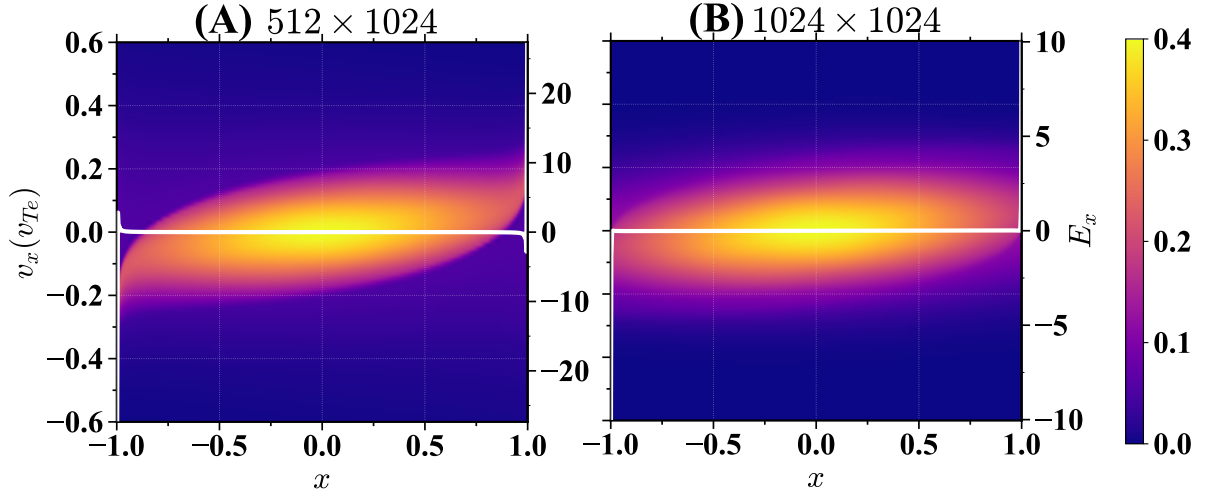


Figure 3: At $t = 25\tau_e$, electron distribution functions and the corresponding spatial electric fields for two grid resolutions:(A) 1024×1024 and (B) 512×1024 .

Conclusion We quantitatively analyze the characteristic temporal and spatial scales for ELM filament transport by identifying the Debye sheath width, l_{sheath} , and the time, τ_{quasi} , for ELM plasma to enter the quasi-neutral state.

- After the filament reaches targets, approximately $7\tau_e - 10\tau_e$ later, the electric field in physical space has only a weak influence on ion transport. During this stage, the ELM plasma has already entered the quasi-neutral regime, and the ions behave approximately as free-streaming particles.
- l_{sheath} is very small, approximately $2\lambda - 3\lambda$. In addition, the sheath electric field is significantly weaker than a self-consistent one.

According to our KOBRA simulations, the ion flux in the whole ELM process is not primarily dominated by the plasma sheath. However, the magnetic field effects and collision probably influences the sheath electric field structure. Therefore, KOBRA will be extended to 1D3V and introduced with magnetic field and collision module in future work. The extended model will be used to quantitatively and qualitatively analyze the effects of magnetic pre-sheath and collisional pre-sheath on ion flux and ion impact energy during ELM. And these effects will be compared with those by self-consistent electric field.

References

- [1] C. J. Wareing et al., Monthly Notices of the Royal Astronomical Society, Vol. 452, No. 2, 1803-1818 (2016)
- [2] G. Manfredi et al., Plasma Physics and Controlled Fusion, Vol. 53, No. 1, 015012 (2010)
- [3] C.-Z. Cheng et al., Journal of Computational Physics, Vol. 22, No. 3, 330-351 (1976)
- [4] P. Degond et al., Journal of Computational Physics, Vol. 229, No. 16, 5630-5652 (2010)